

Genome-Wide Chromatin Immunoprecipitation Sequencing Analysis of the *Penicillium chrysogenum* Velvet Protein PcVelA Identifies Methyltransferase PcLImA as a Novel Downstream Regulator of Fungal Development

Kordula Becker,^a Sandra Ziemons,^a Katharina Lentz,^{a*} Michael Freitag,^b Ulrich Kück^a

Lehrstuhl für Allgemeine und Molekulare Botanik, Ruhr-Universität Bochum, Bochum, Germany^a; Department of Biochemistry and Biophysics, Oregon State University, Corvallis, Oregon, USA^b

ABSTRACT *Penicillium chrysogenum* is the sole industrial producer of the β -lactam antibiotic penicillin, which is the most commonly used drug for treating bacterial infections. In *P. chrysogenum* and other filamentous fungi, secondary metabolism and morphogenesis are controlled by the highly conserved multisubunit velvet complex. Here we present the first chromatin immunoprecipitation next-generation sequencing (ChIP-seq) analysis of a fungal velvet protein, providing experimental evidence that a velvet homologue in *P. chrysogenum* (PcVelA) acts as a direct transcriptional regulator at the DNA level in addition to functioning as a regulator at the protein level in *P. chrysogenum*, which was previously described. We identified many target genes that are related to processes known to be dependent on PcVelA, e.g., secondary metabolism as well as asexual and sexual development. We also identified seven PcVelA target genes that encode putative methyltransferases. Yeast two-hybrid and bimolecular fluorescence complementation analyses showed that one of the putative methyltransferases, PcLImA, directly interacts with PcVelA. Furthermore, functional characterization of PcLImA demonstrated that this protein is involved in the regulation of conidiosporogenesis, pellet formation, and hyphal morphology, all traits with major biotechnological relevance.

IMPORTANCE Filamentous fungi are of major interest for biotechnological and pharmaceutical applications. This is due mainly to their ability to produce a wide variety of secondary metabolites, many of which are relevant as antibiotics. One of the most prominent examples is penicillin, a β -lactam antibiotic that is produced on the industrial scale by fermentation of *P. chrysogenum*. In recent years, the multisubunit protein complex velvet has been identified as one of the key regulators of fungal secondary metabolism and development. However, until recently, only a little has been known about how velvet mediates regulation at the molecular level. To address this issue, we performed ChIP-seq (chromatin immunoprecipitation in combination with next-generation sequencing) on and follow-up analysis of PcVelA, the core component of the velvet complex in *P. chrysogenum*. We demonstrate direct involvement of velvet in transcriptional control and present the putative methyltransferase PcLImA as a new downstream factor and interaction partner of PcVelA.

KEYWORDS: ChIP-seq, PcLImA, PcVelA, *Penicillium chrysogenum*, methyltransferase, protein-DNA interactions, velvet complex

Received 25 May 2016 Accepted 14 June 2016 Published 13 July 2016

Citation Becker K, Ziemons S, Lentz K, Freitag M, Kück U. 2016. Genome-wide chromatin immunoprecipitation sequencing analysis of the *Penicillium chrysogenum* velvet protein PcVelA identifies methyltransferase PcLImA as a novel downstream regulator of fungal development. *mSphere* 1(4):e00149-16. doi: [10.1128/mSphere.00149-16](https://doi.org/10.1128/mSphere.00149-16).

Editor Reinhard Fischer, Karlsruhe Institute of Technology (KIT), Institute for Applied Biosciences

Copyright © 2016 Becker et al. This is an open-access article distributed under the terms of the [Creative Commons Attribution 4.0 International license](https://creativecommons.org/licenses/by/4.0/).

Address correspondence to Ulrich Kück, ulrich.kueck@rub.de.

*Present address: Katharina Lentz, Botanical Institute and Center of Excellence on Plant Sciences (CEPLAS), University of Cologne, Cologne, Germany, and Max Planck Research Group Fungal Biodiversity, Max Planck Institute for Plant Breeding Research, Cologne, Germany.

The discovery of β -lactam antibiotics has rightly been described as one of the most significant milestones in human history, as it enabled effective treatment of bacterial infections for the first time (1). Penicillin, the most commonly used drug within this group of antibiotics, is synthesized by the filamentous ascomycete *Penicillium chrysogenum*, which was first described in 1928 (2). Since then, immense efforts have been made to maximize penicillin yields in large-scale industrial production. For many years, strain improvement programs were based on random mutagenesis approaches, such as treatment with X rays, UV irradiation, and nitrogen mustard mutagenesis (1, 3, 4). One of the main drawbacks of random mutagenesis is that it introduces both desirable and undesirable mutations, and large-scale screening processes are needed to identify the mutant strains with the improved characteristics. Thus, one of the main goals of current strain improvement programs is to replace random mutagenesis with targeted genetic engineering approaches in order to speed and simplify the generation of new strains with properties that help optimize penicillin production. Hence, it is critical to understand the regulation of *P. chrysogenum* morphology, development, and secondary metabolism at the molecular level.

Secondary metabolism and differentiation processes in various filamentous fungi are orchestrated by the multisubunit velvet complex (5–7). The founding member of the complex, VeA (velvet A), was first described as a light-dependent regulator in *Aspergillus nidulans* (8). Subsequent characterization of *veA* deletion and overexpression mutants has confirmed its roles in the regulation of sexual and asexual development, morphogenesis, virulence, and secondary metabolism in several species (6, 7, 9–12). Deletion of the gene for the VeA homologue in *P. chrysogenum* (*PcvelA*) reduces penicillin production and causes light-independent formation of conidiospores. Moreover, the deletion results in dichotomous branching of hyphae and increases pellet formation in shaking cultures (6). Besides *PcvelA*, members of the velvet protein family in *P. chrysogenum* include *PcvelB*, *PcvelC*, and *PcVosA* (13). Furthermore, the putative S-adenosyl-L-methionine (SAM)-dependent methyltransferase (MTase) *LaeA* (loss of *affR* expression A), which acts as a global regulator of secondary metabolism and development in various euascomycetes (6, 7, 14, 15), is also part of the velvet complex. According to our current working model, all of the velvet subunits, together with *PcLaeA*, can interact with at least one other velvet subunit (6, 13). Analyses of a comprehensive set of single- and double-deletion mutants have shown that *PcvelA*, together with *PcLaeA* and *PcvelC*, is an activator of penicillin biosynthesis, whereas *PcvelB* represses this process. Moreover, *PcvelB* and *PcVosA* promote conidiation, while *PcvelC* has an inhibitory effect (6, 13).

Almost 10 years ago, Ni and Yu postulated that velvet proteins might act as global transcriptional regulators, representing a new fungus-specific class of transcription factors (TFs) (16). Supporting evidence for this idea was provided by microarray analyses with *P. chrysogenum* that showed that *PcvelA* influences the expression of 13.6% of all nuclear genes (6). Further, recent RNA-sequencing analyses of *Aspergillus fumigatus* and *A. nidulans* revealed that, respectively, 32% and 26% of all protein-coding genes are regulated in a VeA-dependent manner (17). The first experimental evidence that velvet proteins act as direct regulators at the DNA level was provided for *Histoplasma capsulatum* (18). By chromatin immunoprecipitation with microarray technology (ChIP-chip), two distinct *cis*-acting regulatory sequences were identified, and these are bound directly by Ryp2 and Ryp3, two orthologs of VosA and VeA/VelB, respectively (18). This finding was further supported by structural analyses (19), demonstrating that the velvet domain acts as a DNA-binding domain in *A. nidulans*.

Although extensive efforts were made to decipher the molecular mechanisms that control velvet protein-mediated regulation in various fungi, these mechanisms remain poorly understood. Therefore, the aim of this work was to shed light onto *PcvelA* regulatory functions on a genome-wide scale by using ChIP combined with next-generation sequencing (ChIP-seq). Follow-up analyses were designed to further elucidate *PcvelA* DNA-binding properties on a molecular level and to enable functional characterization of new *PcvelA* downstream factors.

TABLE 1 ChIP-seq design and results

| Sample | No. of reads ^a | No. mapped ^b | % mapped ^c | No. of peaks whose FDR was ≤ 0.001 ^d | No. of differential peaks ^e | No. of total peaks ^f | Estimated fragment length ^g |
|----------------------|---------------------------|-------------------------|-----------------------|--|--|---------------------------------|--|
| PcVelA_shaking_1 | 34,074,601 | 20,835,894 | 61.15 | 6,088 | 1,937 | 764 | 235 |
| PcVelA_shaking_2 | 29,736,045 | 17,177,895 | 57.77 | 6,090 | 1,362 | 1,001 | 231 |
| PcVelA_shaking_input | 20,383,512 | 18,540,910 | 90.96 | | | | |

^aTotal number of sequenced reads.

^bTotal number of reads mapped to the *P. chrysogenum* P2niaD18 genome.

^cFraction of tags found in peaks versus in the genomic background determined by HOMER.

^dNumber of peaks passing the FDR threshold of ≤ 0.001 .

^eNumber of peak regions showing at least a 4-fold enrichment in the ChIP sample over the input DNA.

^fTotal number of peak regions after local background filtering and clonal filtering.

^gEstimated fragment length used for sequencing determined from tag autocorrelation analysis.

RESULTS

Generation of a genome-wide PcVelA DNA-binding profile. Prior to carrying out ChIP experiments, we performed Northern blot hybridization to analyze expression of *PcvelA* under the control of its native promoter sequence and under conditions scheduled for ChIP. As only minimal amounts of the *PcvelA* transcript were detected in the wild-type P2niaD18 and $\Delta Pcku70$ -FRT2 strains (see Fig. S1A in the supplemental material), we decided to use a mutant strain carrying a $P_{gpd}::PcvelA::egfp$ fusion construct for further experiments (Fig. S1B). The corresponding plasmid, pPcVelA-EGFP, was ectopically integrated into *P. chrysogenum* $\Delta PcvelA$, a marker-free *PcvelA* deletion strain. Successful transformation and expression of *PcvelA::egfp* in strain PcVelA-ChIP was verified by PCR, Northern blot, and Western blot analyses (Fig. S1A, S1C, and S1D). Fluorescence microscopy was used to confirm both the presence and the nuclear localization of PcVelA-EGFP (Fig. S1E). The ChIP-seq experiments were performed using two independent biological samples obtained from shaking cultures of strain PcVelA-ChIP. The corresponding data sets were designated PcVelA_shaking_1 and PcVelA_shaking_2. For the input control sample, PcVelA_shaking_input, DNA from strain PcVelA-ChIP was isolated after cell lysis and fragmentation of chromatin by sonication but prior to chromatin immunoprecipitation. As the input DNA went through the whole experimental procedure without any specific enrichment, it represents fractionated genomic DNA. During the bioinformatics analysis, only regions that met the following criteria were regarded as specific PcVelA binding regions: (i) a ≥ 4 -fold enrichment in ChIP DNA over input DNA (ii), a false discovery rate (FDR) threshold of ≤ 0.001 , and (iii) a Poisson *P* value of $\leq 1.00e-04$. We identified 764 and 1,001 regions that were specifically bound by PcVelA in the PcVelA_shaking_1 and PcVelA_shaking_2 data sets, respectively (Table 1).

When we compared the two data sets, only peaks that had a maximum distance of 100 nucleotides (nt) were regarded as overlapping. Doing so, we identified 592 sites that were specifically bound by PcVelA in both biological replicates (see Data Set S1 in the supplemental material). As part of our initial analysis, the peak regions were classified according to their genomic location, i.e., as being close to or within open reading frames (ORFs). A total of 78.9% (467/592) of the peaks showed intergenic localization, while 21.1% (125/592) were located within protein-coding regions. Of the 467 peaks that showed intergenic localization, 39 were within the 3' region of both adjacent ORFs, 225 were 5' of one neighboring gene, and 203 were positioned within divergent promoter regions. Thus, considering only those genes located in the 5'-to-3' orientation with regard to neighboring peak regions, we identified a total of 631 genes that might be controlled directly by PcVelA with high confidence and stringency. Putative binding sites in the 3' region or coding regions may also be used (20), but these are not considered further here. Previous microarray analyses (6) confirmed that 18.9% (119/631) of these genes showed ≥ 2 -fold PcVelA-dependent changes in expression. This overlap is consistent with previous ChIP-seq data from analyses of *P. chrysogenum*, *Saccharomyces cerevisiae*, and higher eukaryotes, which revealed overlaps of 10 to 50% between TF occupancy and the expression of neighboring genes (20–25).

Validation of the PcVelA ChIP-seq data. In order to validate the biological significance of our data set and to rule out bias from the bioinformatics analysis, the PcVelA-specific enrichment of four selected target regions that were identified in the ChIP-seq analyses was confirmed using quantitative ChIP-PCR. Target regions were selected to cover a range of PcVelA binding sites, from high-affinity to midaffinity sites, as deduced from the ChIP-seq data. The enrichment of the target region was calculated as the ratio of the region of interest to the level of a control region showing no PcVelA-specific enrichment in ChIP DNA relative to this ratio in the input DNA. A randomly selected region that showed no specific enrichment in the ChIP-seq data was used as a control (NC). Data from the ChIP-PCR analysis were compared to peak values obtained in the bioinformatics analysis. These values represent the average number of sequence tags found within a peak region after normalization to a total of 10 million mapped tags. The ChIP-PCR results were consistent with the peak values, confirming the specific enrichment of all tested PcVelA target regions (Fig. S2).

Categorization of putative PcVelA target genes. Within our ChIP-seq data set, we identified a remarkably high number of putative PcVelA target genes that were directly related to cellular and developmental processes that are known to be controlled by velvet (Table 2). Most of these genes had shown PcVelA-dependent expression profiles in previous microarray analyses comparing expression levels in a *PcvelA* deletion strain to those in the corresponding $\Delta Pcku70$ wild-type strain (6). However, this was not the case for genes that control conidiation, since this developmental step is most probably regulated at later time points (~120 h). Prominent examples of direct PcVelA target genes include *con-6* (*Pc16g03240*), *flbC* (*Pc12g12190*), *flbD* (*Pc13g03170*), *artA* (*Pc18g03940*), and *brlA* (*Pc23g00400*), all of which are related to different developmental steps of conidiation (26–30). The putative target genes with functions that were related to spore viability and protection included *treA* or *ath1* (*Pc16g11870*), which encodes an α,α -trehalose glucohydrolase, *Pc16g06690*, which encodes a precursor of the spore wall fungal hydrophobin DewA, and *Pc13g09910*, which encodes a late-embryogenesis-abundant (LEA) domain protein (31–33). Interestingly, a PcVelA DNA-binding region was identified within the upstream region of *PcvelB*, a gene that encodes a component of the velvet complex that activates conidiospore formation in various filamentous fungi (5, 7, 13). However, *PcvelB* did not show PcVelA-dependent expression in previous microarray analyses, and the peak value of the corresponding ChIP-seq peak region suggested a rather low-affinity target region. In addition to identifying genes related to conidiation and development, we identified several genes that encoded proteins related to various aspects of secondary metabolism, such as *Pc21g08920*, which encodes a norsolorinic acid reductase, *Pc21g12630*, which encodes a nonribosomal peptide synthetase, and *stuA* (*Pc13g04920*), which encodes a TF with a basic helix-loop-helix domain. Notably, *StuA* not only regulates penicillin biosynthesis in *P. chrysogenum* (34) but also controls asexual reproduction, especially conidiophore development, in *A. nidulans* (35).

Genes that are related to known velvet-regulated functions were localized next to some of the peaks with the highest peak values. It is generally accepted that the regions that are identified by ChIP-seq analysis with DNA-binding proteins are positioned next to known functional target genes (36). However, ChIP-seq analysis also identified a large number of highly significant PcVelA target regions next to genes that have not previously been associated with PcVelA or with any other component of the velvet complex. We identified, among other genes, numerous genes that encode uncharacterized TFs, which may act as downstream factors of PcVelA. In Table 2, we included only those TF genes that showed PcVelA-dependent expression in a microarray analysis. This observation is consistent with ChIP-seq data obtained with the *Neurospora crassa* circadian regulator white collar complex (WCC), revealing that the protein directly controls the expression of 24 TFs, which in turn might be involved in transcriptional control on a second hierarchical level (20). Furthermore, we also identified seven genes encoding putative MTases.

TABLE 2 Selected PcVela target genes identified in ChIP-seq analyses^d

| Protein coding category and locus tag | Description ^a | Relevant characteristic(s) | Peak value(s) ^b | Microarray result for Δ PcvelA strain ^c | | |
|---------------------------------------|---|---|----------------------------|---|------|------|
| | | | | 48 h | 60 h | 96 h |
| Development and conidiation proteins | | | | | | |
| <i>Pc18g03940</i> | 14-3-3 Family protein ArtA | Overexpression causes a severe delay in the polarization of conidiospores in <i>A. nidulans</i> (28) | 1,090 | -0.1 | 0 | -0.1 |
| <i>Pc13g04920</i> | Cell pattern formation-associated protein StuA | Inactivation reduces expression of the penicillin gene cluster in <i>P. chrysogenum</i> (34); required for differentiation and spatial organization of cell types of the <i>A. nidulans</i> conidiophore (35) | 1,034 | -0.1 | 0.4 | -0.1 |
| <i>Pc13g09580</i> | bZIP transcription factor AtfA | Deletion mutant conidia show significant sensitivity to high temperature and oxidative stress in <i>A. fumigatus</i> (69); the protein regulates different types of stress responses in <i>A. nidulans</i> (70) | 1,027 | -0.9 | -0.7 | -1.1 |
| <i>Pc16g03240</i> | Conidiation protein con-6 | Expressed during the formation of asexual spores or after illumination of vegetative mycelia in <i>N. crassa</i> (30) | 801 | 0.9 | 0.8 | 0.3 |
| <i>Pc16g11870</i> | α,α -Trehalose glucohydrolase TreA/Ath1 | Gene product is localized in the conidiospore wall; it is required for growth on trehalose as a carbon source in <i>A. nidulans</i> (31) | 761 | -0.1 | -0.2 | -0.3 |
| <i>Pc21g09870</i> | Related to integral membrane protein Pth11 | Functions at the cell cortex as an upstream effector of appressorium differentiation in <i>M. grisea</i> (71) | 746 | 0 | 1.5 | 1.6 |
| <i>Pc16g06690</i> | Spore wall fungal hydrophobin DewA precursor | Encodes a fungal hydrophobin component of the conidial wall (32) | 730 | -0.1 | 0.2 | -0.2 |
| <i>Pc12g12190</i> | C ₂ H ₂ conidiation transcription factor FlbC | Putative nuclear TF necessary for proper activation of conidiation, growth, and development in <i>A. nidulans</i> (29) | 613 | -0.5 | 0.3 | -0.2 |
| <i>Pc13g09910</i> | LEA (late-embryogenesis-abundant) domain protein | Associated with tolerance to water stress resulting from desiccation and cold shock in plants and animals (33, 72) | 560 | -0.6 | 0 | -0.8 |
| <i>Pc13g03170</i> | MYB family conidiophore development protein FlbD | Regulates both asexual and sexual differentiation in <i>A. nidulans</i> (27) | 553 | 0.9 | 0.5 | 0.2 |
| <i>Pc22g22320</i> | Developmental regulator VelB | Acts as an activator of conidiospore formation in various filamentous fungi (5, 13) | 506 | 0.2 | 0.6 | 0.4 |
| <i>Pc23g00400</i> | C ₂ H ₂ -type conidiation transcription factor BrIA | Mediates developmental switch from apical growth of vegetative cells to budding growth pattern of conidiophores (26) | 396 | -0.1 | 1.2 | 0.2 |
| Secondary metabolism proteins | | | | | | |
| <i>Pc22g06500</i> | Amino acid transporter | | 2,544 | 0.9 | 1.0 | 1.2 |
| <i>Pc22g17530</i> | ABC multidrug transporter aa5 | | 2,154 | 0 | -0.3 | 1.5 |
| <i>Pc22g06610</i> | Neutral amino acid permease | | 1,585 | 0.2 | 0.6 | 1.4 |
| <i>Pc20g05090</i> | ABC multidrug transporter | | 1,262 | 1.0 | 0.4 | 0.2 |
| <i>Pc16g11480</i> | PKS, putative | | 870 | -2.7 | -3.7 | -4.3 |
| <i>Pc16g11470</i> | ABC multidrug transporter | | 870 | 0.3 | -1.2 | 0.5 |
| <i>Pc20g03900</i> | MFS multidrug transporter | | 716 | 0.4 | 1.2 | 1.3 |
| <i>Pc18g00380</i> | Hybrid NRPS PKS | | 644 | 0.1 | 0.5 | 0.1 |
| <i>Pc21g12630</i> | NRPS | | 621 | -2.6 | -1.5 | -0.1 |
| <i>Pc20g12260</i> | ABC drug exporter AtrF | | 538 | 0.3 | 0.7 | 1.1 |
| <i>Pc12g14890</i> | MFS multidrug transporter | | 538 | 0.3 | 0.8 | 3.4 |
| <i>Pc22g22420</i> | MFS transporter | | 528 | 1.3 | 1.5 | 4 |
| <i>Pc18g03610</i> | ABC multidrug transporter | | 481 | -0.1 | 0 | 2.8 |
| <i>Pc18g03610</i> | ABC multidrug transporter | | 481 | -0.1 | 0 | 2.8 |
| <i>Pc21g08920</i> | Norsolorinic acid reductase | | 343 | -0.2 | 0.5 | 1.9 |
| Transcription factors | | | | | | |
| <i>Pc20g05960</i> | C ₂ H ₂ transcription factor | | 1,705 | -0.7 | -1.0 | -1.7 |
| <i>Pc21g15330</i> | bZIP TF | | 1,040 | -1.2 | -1.1 | -1.9 |
| <i>Pc06g02030</i> | C ₂ H ₂ finger domain protein | | 986 | -3.1 | -3.2 | -2.3 |
| <i>Pc15g00130</i> | F-box domain protein | | 885 | -1.0 | -0.2 | -0.9 |
| <i>Pc21g15330</i> | bZIP TF | | 725 | -1.2 | -1.1 | -1.9 |
| <i>Pc12g10080</i> | C6 finger domain protein | | 576 | -1.4 | -0.6 | 0 |

(Continued on following page)

TABLE 2 (Continued)

| Protein coding category and locus tag | Description ^a | Relevant characteristic(s) | Peak value(s) ^b | Microarray result for Δ PcvelA strain ^c | | |
|---------------------------------------|--|--|----------------------------|---|------|------|
| | | | | 48 h | 60 h | 96 h |
| Methyltransferases | | | | | | |
| <i>Pc21g02240</i> | LaeA-like SAM-dependent methyltransferase PCLImA | | 2,756 | 2.6 | 1.6 | 0.8 |
| <i>Pc18g01840</i> | LaeA-like SAM-dependent methyltransferase PCLImB | Part of a membrane-associated trimeric complex that controls a signal transduction pathway for fungal differentiation in <i>A. nidulans</i> (41) | 2,139, 1,430 | -2.6 | -2.1 | -1.7 |
| <i>Pc21g12700</i> | SAM-dependent methyltransferase | | 1,101 | -1.4 | -0.4 | 0.5 |
| <i>Pc18g04780</i> | SAM-dependent methyltransferase | | 660 | 0.1 | 0.6 | 0.6 |
| <i>Pc18g06010</i> | O-Methyltransferase | | 470 | 0.1 | 0 | 0.1 |
| <i>Pc13g15570</i> | Nicotinamide N-methyltransferase | | 334 | 0.8 | 0.7 | 1.0 |
| <i>Pc22g01170</i> | O-Methyltransferase | | 328 | 4.5 | 4.6 | 4.5 |

^aAs obtained from blastp analysis (<http://blast.ncbi.nlm.nih.gov/Blast.cgi>).

^bThe statistical peak value is the average tag count found at peak normalized to 10 million total mapped tags.

^cMicroarray data showing expression changes in the Δ PcvelA strain relative to expression in the wild-type Δ Pcku70 strain after 48, 60, and 96 h of cultivation (6).

^dFor comparison, previously obtained expression data from microarray hybridizations (6) are shown. Upregulated genes are marked by red shading, and downregulated genes are marked by green shading. PcVelA target genes within each category are arranged based on peak values obtained from bioinformatics ChIP-seq analysis. High peak values indicate strong binding of PcVelA to the respective 5' region. NRPS, nonribosomal peptide synthetase; PKS, polyketide synthase; MFS, major facilitator superfamily.

De novo prediction and validation of a PcVelA DNA-binding motif. We used the MEME (Multiple Expression Motifs [EM] for Motif Elicitation) platform to perform *de novo* prediction of a PcVelA DNA-binding motif based on the peak regions obtained in the ChIP-seq experiments. Our analysis revealed one highly significant motif sequence, designated PcVelA.M1 (Fig. 1A), that was present in 275 (46.5%) out of 592 peak regions using a statistical threshold of a *P* of ≤ 0.001 . While a comparison of PcVelA.M1 to known binding motifs in the JASPAR CORE (2014) fungi database did not reveal any significant matches, comparison to the JASPAR CORE (2014) vertebrate database revealed some interesting similarities to other motifs. As shown in Fig. S3 in the supplemental material, PcVelA.M1 most closely resembled the DNA-binding motifs of NR2E3, a TF involved in human photoreceptor development (37, 38), and NR2F1, a nuclear hormone receptor and transcriptional regulator that plays an important role in the neurodevelopment of the visual system in humans (39). Independently of the bioinformatics analysis, we also noticed strong similarity between PcVelA.M1 and the DNA-binding motif sequence described for the Ryp2/Ryp3 heterodimer from *H. capsulatum* (18) as well as weak similarity to a DNA-binding consensus sequence that was recently described for *A. nidulans* VosA (19).

To further verify the biological significance of PcVelA.M1, we performed electrophoretic mobility shift assays (EMSAs) using a glutathione S-transferase (GST)-tagged version of the PcVelA N-terminal region from amino acids 1 to 256 (PcVelA₁₋₂₅₆), which was purified from *Escherichia coli*, and 50-nt DNA sequences (PCLImA_2 and PCLImA_4) derived from a region within the PCLImA upstream sequence (Fig. 1B). Both oligonucleotides contained exactly one copy of PcVelA.M1 and showed specific binding to PcVelA₁₋₂₅₆ (Fig. 1C). Specific binding was also documented for full-length PcVelA (Fig. S4); however, the PcVelA N terminus seemed to be sufficient for effective DNA binding. As PcVelA₁₋₂₅₆ includes the complete velvet domain, this might indicate that the velvet domain mediates DNA binding, as demonstrated for *A. nidulans* VosA and VelB (19). The specificity of the binding between PcVelA and the DNA-binding consensus sequence PcVelA.M1 was further verified by testing the binding of mutated versions of the PCLImA_2 and PCLImA_4 oligonucleotides (Fig. 1C and D) to PcVelA₁₋₂₅₆. Formation of protein-DNA complexes was drastically reduced when mutations were introduced into the motif sequence. This observation supports our hypothesis that

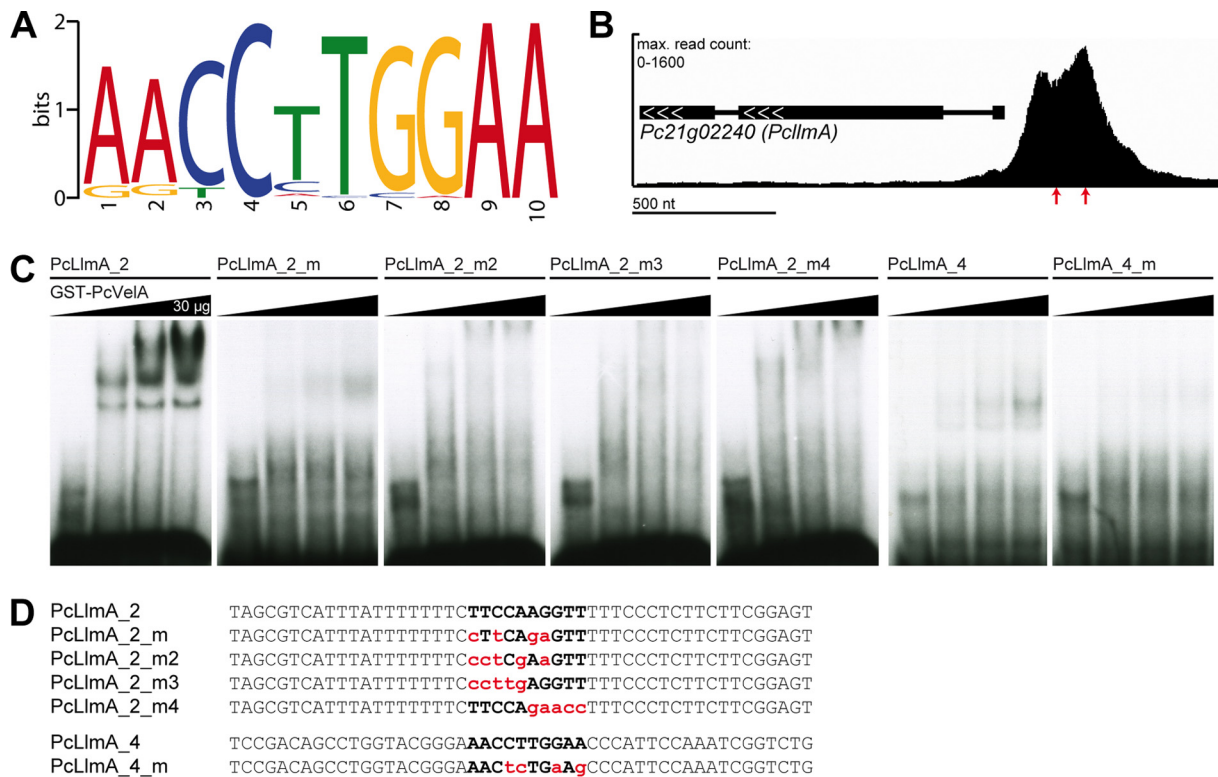


FIG 1 Electrophoretic mobility shift assays (EMSA) confirm PcVela binding to the predicted DNA-binding consensus sequence PcVela.M1. (A) PcVela-specific peak regions were submitted to MEME (63) for *de novo* motif prediction. Only the most significant putative DNA-binding motif, PcVela.M1, is shown. The size of each letter is proportional to the frequency of each nucleotide at this position within the consensus sequence. (B) Enlargement of ChIP-seq profile from PcVela_shaking_1 next to *Pc21g02240*, encoding the putative SAM-dependent MTase PcLlmA. Positions of oligonucleotides, which were used for shift analysis, are indicated by red arrows. (C) EMSAs were performed using 50-nt radiolabeled double-stranded oligonucleotide probes (PcLlmA_2, PcLlmA_4) derived from the *PcLlmA* promoter region and increasing amounts of purified GST-PcVela₁₋₂₅₆ protein. Application of mutated versions of PcLlmA_2 and PcLlmA_4 resulted in reduced formation of protein-DNA complexes. (D) Sequences of oligonucleotide probes used for the experiment whose results are shown in panel C. The PcVela.M1 binding sequence is indicated with bold letters. Mutated bases are lowercase and red.

PcVela.M1 is necessary and sufficient to mediate DNA binding of PcVela to its specific target sites.

Further characterization of putative MTases. We found that five of the seven genes that encoded putative MTases in the PcVela ChIP-seq data set showed significant PcVela-dependent expression profiles in previous microarray analyses (Table 2) (6). Because recent reports from other eukaryotes point to a functional link between VeA homologs and several putative MTases (40–42), we focused further analyses on this group of new PcVela target genes. First, we performed quantitative reverse transcription-PCR (qRT-PCR) analysis to validate the PcVela-dependent expression of MTase-encoding genes. We compared expression levels in strain PcVela-ChIP, which is characterized by elevated *PcvelA* expression, and the $\Delta PcvelA$ strain with levels in wild-type P2niaD18. As a reference for normalization, we used amplification of a fragment of the 18S rRNA. All strains were grown under the same conditions as for ChIP-seq sample preparation. As shown in Fig. 2, PcVela-dependent expression profiles were confirmed for four out of seven tested MTase genes, namely, *PcLlmA* (*Pc21g02240*), *PcLlmB* (*Pc18g01840*), *Pc21g12700*, and *Pc22g01170*. *Pc18g06010* showed PcVela-dependent expression in qRT-PCR but not in microarray analysis (Table 2). Next, the amino acid sequences of the putative MTases were compared to the sequences of PcLaeA, a putative methyltransferase that is part of the velvet complex, as well as *A. nidulans* LlmF, VapB, and VipC (homolog of PcLlmB), which have previously been described as velvet-associated proteins (40, 41). In general, a set of three conserved sequence motifs (motifs I to III) that are essential for catalytic activity are found in most MTases (43, 44). The most prominent one, motif I, is characterized by the glycine

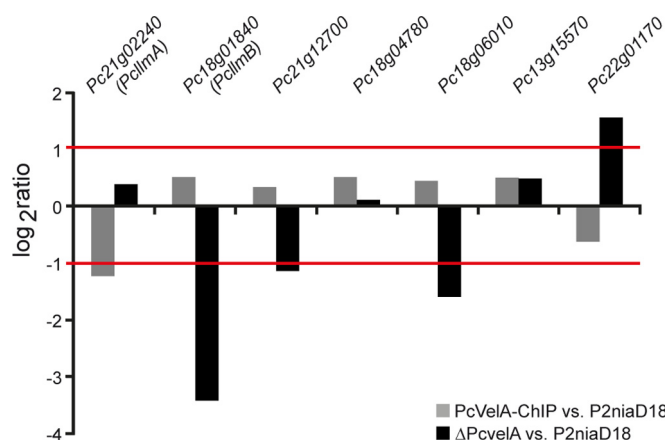


FIG 2 qRT-PCR analysis confirms PcVelA-dependent expression of putative MTase-encoding genes. Analysis of relative log₂-fold gene expression ratios of putative MTase-encoding genes confirmed PcVelA dependency. Ratios of their expression in PcVelA-ChIP (gray bars) and the ΔPcvelA strain (black bars) are shown compared to that in wild-type P2niaD18. Values are the mean scores from three biological replicates. Partial amplification of the 18S rRNA was used as a reference for normalization.

(G)-rich sequence E/DXGXGXG, which is conserved in fungi, plants, and humans (41, 45, 46). Overall comparison of amino acid sequences revealed that PcLlmA, PcLlmB, and PcLaeA, as well as LlmF, VapB, and VipC from *A. nidulans*, had only moderate similarity (Fig. S5A). However, the region spanning SAM-binding motif I was highly conserved, as were several amino acid residues that are involved in SAM binding (45, 46). This degree of conservation is also found for other SAM-dependent MTases, which generally share a set of conserved MTase sequence motifs plus a highly conserved structural fold but show rather low overall sequence similarity (43, 44, 46).

PcLlmA shows the typical SAM-MTase fold. Because we identified *PcLlmA* as a direct target gene of PcVelA and because the SAM-binding domains of PcLlmA and other velvet-associated MTases were highly conserved (Fig. S5A), we continued to functionally characterize the protein. First the PcLlmA amino acid sequence was submitted to the I-TASSER server (47–49) to predict the secondary structure of the protein. As shown in Fig. S5B, PcLlmA has the typical SAM-dependent MTase fold, which is characterized by alternating α -helices (α 1 to α 8) and β -strands (β 1 to β 7) that form a seven-stranded β -sheet (46). The highly conserved glycine-rich sequence E/DXGXGXG (motif I) and the conserved amino acid residues that are involved in SAM binding (45, 46) localize to the SAM-binding N-terminal region of the protein, whereas the substrate-binding region of the protein is located at the C terminus of the β -sheet.

PcLlmA directly interacts with PcVelA in the nucleus. Next we focused on direct interactions between PcLlmA and components of the velvet complex. As shown in Fig. 3A, we confirmed that there was a direct interaction between PcVelA and PcLlmA using an *ex vivo* yeast two-hybrid (Y2H) approach. Briefly, diploid yeast strains that synthesize both the bait and the prey proteins were spotted on selective media that lacked adenine and histidine (in order to select for *ADE2* and *HIS3*) and that were supplemented with X- α -Gal (5-bromo-4-chloro-3-indolyl- α -D-galactopyranoside; to demonstrate *lacZ* reporter gene activity). Only those interactions that could be verified based on both reporter systems (growth on selective media and blue color) were considered positive. Interestingly, PcLlmA interacted with PcVelA but not with the other velvet components, i.e., PcVelB, PcVelC, PcVosA, or the putative MTase PcLaeA (Fig. 3A; Fig. S6). To confirm the interaction between PcVelA and PcLlmA *in vivo* and in the homologous system, we used bimolecular fluorescence complementation analysis (BiFC) (50). Genes encoding PcVelA and PcLlmA were fused to *eyfp* fragments encoding either the N or the C terminus of the yellow fluorescent protein (YFP), and strains harboring both constructs were analyzed using fluorescence microscopy. As a control,

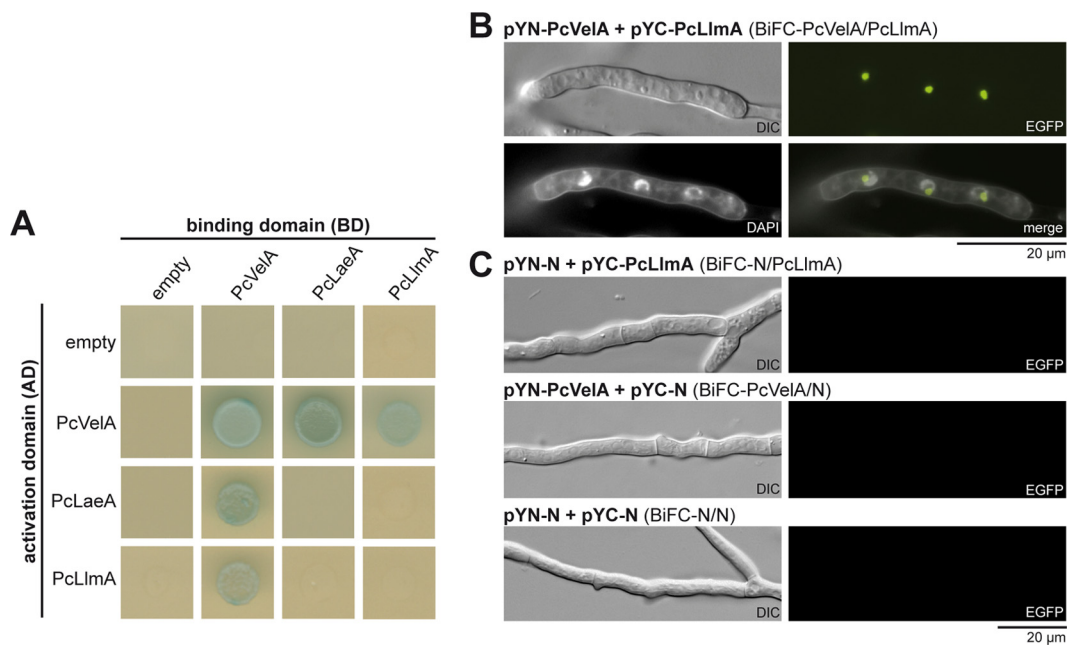


FIG 3 PcVelA directly interacts with the putative SAM-dependent MTase PclImA. (A) For yeast two-hybrid analysis, diploid yeast strains were spotted on selective media that lacked adenine and histidine (in order to select for *ADE2* and *HIS3*) and that were supplemented with X- α -Gal (to demonstrate *lacZ* reporter gene activity). (B) For BiFC analysis, genes encoding PcVelA and PclImA were fused to *eyfp* fragments encoding either the N or the C terminus of the yellow fluorescent protein, and strains harboring both constructs were analyzed using fluorescence microscopy. DAPI staining confirmed the nuclear localization of the PcVelA-PclImA interaction. (C) As a control, strains generating either both split YFPs or one split YFP together with EYFP-PcVelA/PclImA-EYFP are shown. Scale bar = 20 μ m.

we investigated strains that generated only split enhanced YFPs (EYFPs) and strains producing one split EYFP together with either EYFP-PcVelA or PclImA-EYFP. As shown in Fig. 3B, strains carrying both *PcvelA-eyfp* and *PclImA-eyfp* fusion constructs showed clear EYFP signals, while no fluorescence was detectable in control strains (Fig. 3C). DAPI (4',6-diamidino-2-phenylindole) staining demonstrated that the interaction between PcVelA and PclImA occurs in the nucleus (Fig. 3B), as was shown previously for the interaction between PcVelA and PcLaeA, PcVelB, PcVelC, and PcVosA as well as for the interaction of PcVelA with itself (6, 13).

Functional characterization of the putative SAM-dependent MTase PclImA. To further analyze the regulatory properties of PclImA, marker-free *PclImA* deletion, complementation, and overexpression strains were generated and verified using PCR, Southern blot, and qRT-PCR analyses. While the mutant strains showed no significant phenotypes in terms of penicillin biosynthesis efficiency or stress tolerance, there were marked differences in levels of conidiosporogenesis, pellet formation, and hyphal morphology compared to those of the wild-type strain. In all analyses, complementation of the deletion mutants with *PclImA* under the control of its native promoter sequence at its native locus restored the wild-type phenotypes.

As shown in Fig. 4, Δ *PclImA* strains showed almost no changes in their conidiospore formation rates compared to the corresponding wild-type Δ *Pcku70-FRT2* strain under dark and light conditions. In contrast, the *PclImA* overexpression mutants were characterized by significantly elevated conidiospore formation compared to that of the corresponding wild-type strain P2niaD18, indicating that PclImA acts as a positive regulator of asexual development in *P. chrysogenum*. Conidiosporogenesis in these strains still showed light dependency, resulting in the formation of more spores when the organisms were grown under light versus dark conditions. These results are in line with previous studies of *A. nidulans*, demonstrating that overexpression of *IlmF*, encoding a putative SAM-dependent MTase similar to PclImA, results in an increased formation of conidiospores but that deletion of *IlmF* has no effect on asexual devel-

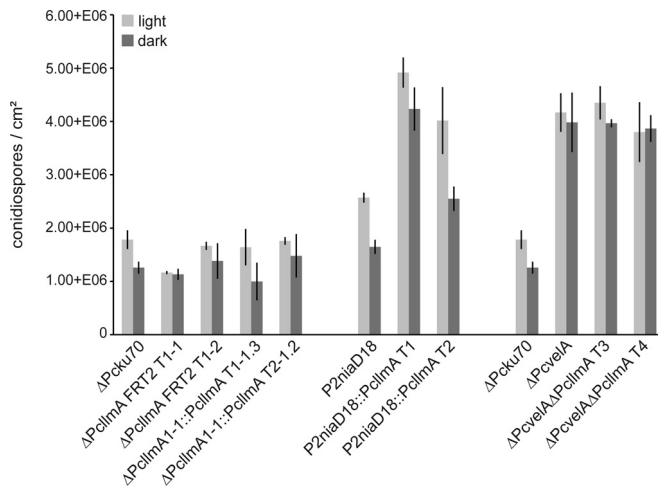


FIG 4 Quantitative analysis of conidiospore formation. Sporulation rates (numbers of conidiospores per cm²) are given for cultures grown for 120 h at 27°C under constant light (light bars) and constant dark (dark bars) conditions, respectively. Values are the mean scores from three biological replicates; averages ± standard deviations are indicated.

opment in this fungus (40). To further test whether PclImA functions downstream of PcVeIA, we investigated sporulation characteristics of ΔPcveIA ΔPclImA double mutants. The sporulation phenotype of these strains resembled the phenotype observed previously for the ΔPcveIA strain, a strain that is characterized by elevated light-independent formation of conidiospores. These results support the idea that PclImA acts downstream of PcVeIA.

When pellet formation was analyzed in shaking cultures, again, we found that the deletion of PclImA did not result in specific phenotypic changes. However, PclImA overexpression led to a dramatic increase in pellet diameter (Fig. 5). About 35% of the pellets in these strains had diameters of ≥1,500 μm, whereas only ~2% of the pellets in the recipient P2niaD18 strain were that large. Notably, this phenotype resembled the one described previously for the ΔPcveIA strain, which is characterized by the formation of larger and more-stable pellets than are formed by the corresponding wild-type strain

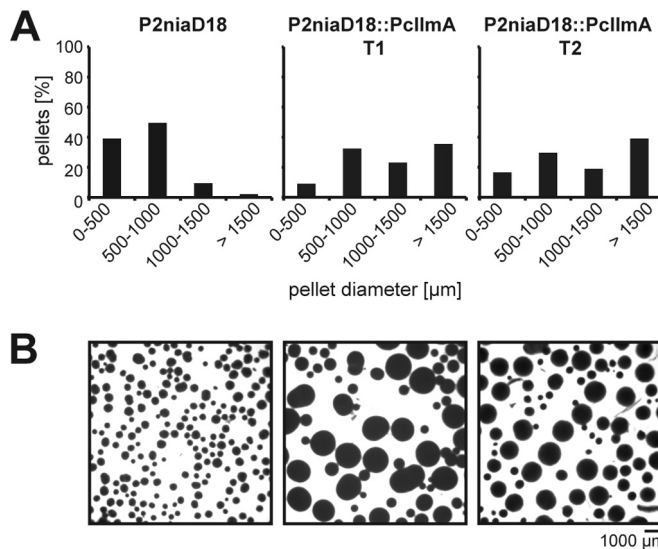


FIG 5 Quantification of pellet formation. (A) Distribution of pellet diameters after 72 h in liquid shaking cultures; (B) representative micrograph for each culture analyzed in panel A. Scale bar = 1,000 μm.

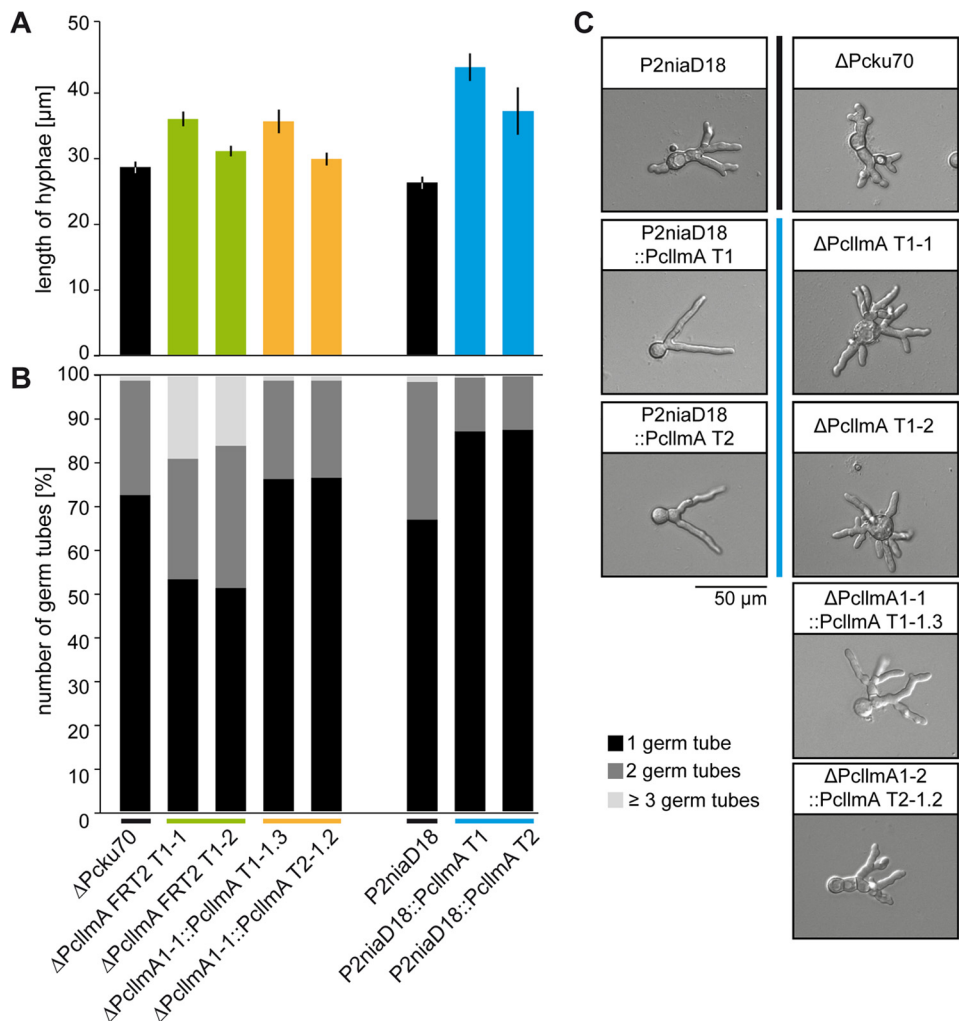


FIG 6 Hyphal morphology of germinating conidia. (A) Lengths of germinating hyphae were measured after 18 h of cultivation on solid CCM. Values are the mean scores of 300 independent measurements; averages \pm standard deviations are indicated. (B) Numbers of germ tubes per germinating conidiospore were determined for 300 independent spores after 18 h of cultivation on solid CCM. Values are given as percentages of all analyzed hyphae per strain. Black, 1 germ tube; dark gray, 2 germ tubes; light gray, ≥ 3 germ tubes per conidiospore. (C) Representative micrographs of germinating conidiospores analyzed in panels A and B. Scale bar = 50 μ m.

(6). To better understand the origin of the observed phenotypic changes, we performed microscopic analysis of germinating conidiospores from *PcllMA* overexpression and deletion strains as well as from the corresponding $\Delta Pcku70$ -FRT2 and P2niaD18 reference strains. As shown in Fig. 6A and C, *PcllMA* overexpression mutants showed increased germ tube length, whereas $\Delta PcllMA$ strains showed no significant differences from the wild-type phenotype. However, when we focused on the number of hyphae that were emerging from the conidiospores, we found that the deletion strains were characterized by an increased formation of germ tubes with extensively branching tips. Specifically, $\sim 20\%$ of the germinating conidiospores formed ≥ 3 germ tubes versus $\sim 2\%$ in the recipient $\Delta Pcku70$ -FRT2 strain. In contrast, the overexpression mutants showed fewer germ tubes, and these tubes lacked terminal branching. Specifically, $\sim 90\%$ of the germinating conidiospores formed only 1 germ tube versus $\sim 65\%$ in the recipient P2niaD18 strain (Fig. 6B and C).

Taken together, these data show that *PcllMA* controls not only asexual development but also pellet formation and the germination characteristics of *P. chrysogenum*. This observation is important, as a direct connection between putative MTases and

hyphal and pellet morphology has been described for PcLaeA (6) but not for any other putative MTase in any other filamentous fungus until now.

DISCUSSION

In recent years, characterization of the velvet complex components has been the focus of molecular genetic research in filamentous fungi (5–7). However, the molecular mechanisms underlying velvet-mediated regulation have remained unclear. In this report, we present the first ChIP-seq analysis of one of the core components of the velvet complex and provide evidence for the involvement of PcVelA in genome-wide transcriptional regulation at the DNA level. Furthermore, we introduce PcLlmA, a putative SAM-dependent MTase, as a downstream factor and direct interaction partner of PcVelA, which is involved in the regulation of developmental processes, such as conidiosporogenesis, pellet formation, and hyphal morphology.

PcVelA acts as a regulator at the DNA level. Most importantly, our work provides evidence that the regulatory functions of PcVelA are not restricted to protein-protein interactions with other velvet components but most likely include regulatory functions directly at the DNA level. In total, we identified 592 specific PcVelA-binding sites that showed distribution all over the *P. chrysogenum* genome. This observation is in agreement with an earlier hypothesis that the velvet proteins might act as global transcriptional regulators, representing a new fungus-specific class of TFs (16). Furthermore, our results are supported by recent data obtained with *H. capsulatum* and *A. nidulans* which demonstrated direct interaction between velvet proteins and DNA (18, 19, 51). ChIP-chip analysis of *H. capsulatum* revealed that Ryp2 and Ryp3, homologs of VosA and VeA/VelB, respectively, show genome-wide association with a total of 361 sites throughout the genome (18). Similarly, ChIP-chip and ChIP-PCR analysis proved that VosA from *A. nidulans* binds to more than 1,500 sites within the genome (19). ChIP-PCR analysis demonstrated further that VeA from *A. nidulans* binds DNA together with the blue-light TF LreA, in order to control light-dependent gene expression (51).

Using *in silico* prediction followed by EMSA, we identified a specific 10-nt PcVelA DNA-binding motif (PcVelA.M1), defined by the consensus sequence AACCTTGGA, which was present in 46.5% of all PcVelA peak regions ($P \leq 0.001$). The sequence shows strong similarity to the DNA-binding motif sequence described for the Ryp2/Ryp3 heterodimer (GAACCATGGT) (18) as well as moderate similarity to the DNA-binding motif sequence previously described for VosA (GCCTTGCCAG) (19). Interestingly, comparison of PcVelA.M1 to the JASPAR CORE (2014) fungi database did not reveal any significant matches. Taken together, these observations provide further evidence for the idea that velvet proteins might represent a new class of fungal TFs which share similar DNA-binding properties. It remains unclear if or to what extent formation of homo- and heterodimers between velvet proteins and other factors affects their ability to specifically bind to DNA. For example, DNA-binding studies with Ryp2 and Ryp3 were successful only when a combination of both proteins was used, whereas both proteins alone did not show any binding to DNA. Similarly to that, *A. nidulans* VosA and VeA are able to bind DNA by themselves, whereas VelB binds as a heterodimer only with VosA *in vitro* (19). However, using ChIP-PCR analysis, Hedtke et al. (51) showed that VeA binding to DNA is dependent on phytochrome FphA, which, however, does not bind to DNA itself. VeA in turn is required for DNA binding of the blue-light TF LreA (51).

The putative MTase PcLlmA acts as a downstream factor and interaction partner of PcVelA. This study identified a remarkable number of putative PcVelA target genes that showed a direct association with processes that are regulated by velvet proteins, such as conidiation, development, and secondary metabolism. Interestingly, we also identified at least seven putative MTase genes as targets of PcVelA. A protein encoded by one of these genes, the putative SAM-dependent MTase PcLlmA, was identified as a downstream factor of PcVelA based on data obtained from ChIP-seq and qRT-PCR experiments. While overexpression of *PcLlmA* affected conidiosporogenesis, pellet formation, hyphal morphology, and germination characteristics, deletion of the gene resulted in phenotypic changes only within the context of conidiospore

germination. Interestingly, the observed changes in asexual sporulation are not dependent on BrlA or PcVelA, as expression of the corresponding genes is not effected in the *PcLlmA* deletion and overexpression strains. As part of the functional characterization of *PcLlmA*, Y2H and BiFC analysis revealed direct interaction between PcVelA and *PcLlmA* at the protein level. This interaction seemed to be restricted to PcVelA, as no interactions between *PcLlmA* and other components of the velvet complex were detected. This observation is consistent with the results of previous Y2H analyses which found that the interaction between the putative MTase *PcLaeA* and components of the velvet complex was mediated solely by PcVelA (13). Furthermore, DAPI staining confirmed the nuclear localization of PcVelA-*PcLlmA* *in vivo*, which was described previously for PcVelA-*PcLaeA* and PcVelA-*PcVelB* (6), PcVelA-*PcVelC* and PcVelA-*PcVosA* (13), and VeA-*LlmF* (40), VeA-*VipC*, and *VipC-VapB* in *A. nidulans* (41). These observations suggest an important role for PcVelA in velvet-mediated regulatory functions in cooperation with a variety of putative MTases.

Notably, the interactions between VeA and putative MTases other than *LaeA* are not restricted to *P. chrysogenum*; rather, they seem to be a common feature of filamentous ascomycetes (52). For example, in *A. nidulans*, the *LlmF* MTase is involved in VeA localization, and the *VipC* and *VapB* MTases are involved in regulating sexual and asexual development (40, 41). In *Fusarium graminearum*, the velvet protein *FgVeA* interacts in a Y2H screen with a total of six putative MTases (42). It remains unclear how the interactions between VeA and the growing number of MTases are mediated at the structural level. Some suggest that VeA may have an affinity domain for MTases or a tertiary domain that interacts with MTases (5, 41). Experimental evidence is needed to confirm these hypotheses and to elucidate the functional consequences of these interactions in greater detail. Moreover, it will be highly interesting to see if *PcLlmA* has any protein MTase activity, which would make it one of the most promising PcVelA interaction partners identified so far. Similar functions have been hypothesized for *LaeA* and *VapB*, but experimental evidence for their direct involvement in protein methylation, let alone genome-wide chromatin modification, is lacking. When considering the functions of *PcLaeA*, *VapB*, and even *PcLlmA* at the molecular level, it should be noted that the biological roles of SAM-dependent MTases are versatile. Specifically, these proteins catalyze the transfer of methyl groups from SAM to a large variety of acceptor substrates that range from small metabolites to bio-macromolecules, including DNA, proteins, and secondary metabolites (42, 46, 53). On the one hand, this makes them highly interesting candidates for biotechnology applications (53); on the other hand, this emphasizes why researchers must consider the possibility that SAM-dependent MTases may have numerous functions besides those involved in the epigenetic modification of chromatin.

Conclusions. This study provides important insights into the regulatory functions of PcVelA on a genome-wide scale. The data presented here revealed that PcVelA is both a transcriptional regulator and a core component of the multisubunit velvet complex. The protein's exceptional position as a scaffold that connects velvet proteins, putative MTases, and DNA will be investigated in greater detail in future studies. In addition, this work identified the putative MTase *PcLlmA* as a new interaction partner of PcVelA and as a regulator of conidiosporogenesis, pellet formation, and hyphal morphology in *P. chrysogenum*. Additional studies are needed to elucidate the molecular mechanisms underlying the regulatory functions that are mediated by this newly discovered MTase.

MATERIALS AND METHODS

Strains and culture conditions. *Penicillium chrysogenum* strains (see Table S1 in the supplemental material) were grown in conditioned culture medium (CCM) (54) with shaking or as surface cultures at 27°C. For inoculation, we used 0.5×10^7 spores derived from cultures grown on M322 solid medium (54) for 4 to 5 days. *Escherichia coli* strain XL1-Blue was used for cloning and plasmid propagation purposes, while BL21(DE3) served as a host for heterologous overexpression of PcVelA-GST (55, 56). *Saccharomyces cerevisiae* strains PJ69-4a and PJ69-4 α were used for yeast two-hybrid analysis (57). Strains were grown at 30°C on synthetic defined (SD) medium lacking selected amino acids used for auxotrophy marker

selection. Mating of the PJ69-4a and α strains was performed in liquid yeast extract-peptone-dextrose agar (YPDA) medium at 30°C and 50 rpm.

Construction of *P. chrysogenum* strains. Strains were constructed by ectopic or homologous integration of plasmid DNA (see Table S2 in the supplemental material) as described previously (6, 58), with some modifications. Recipient strains were grown for 72 h in shaking cultures, and protoplasts were transformed with either circular (for ectopic integration) or linear (for homologous recombination) plasmid DNA. Transformants were selected on CCM containing 150 μ g/ml nourseothricin (Werner BioAgents, Germany). Resistant colonies were isolated and tested for integration of plasmid DNA. PCR analysis and SDS-PAGE–Western blot analysis were performed as described previously (6).

Nucleic acid isolation, cDNA synthesis, qRT-PCR, and ChIP-PCR. Isolation of nucleic acids, cDNA synthesis, qRT-PCR, and ChIP-PCR analysis were carried out as described earlier (25, 59, 60). A fragment of the 18S rRNA amplified using oligonucleotides SSU1 and SSU2 was used as a reference for normalization. Oligonucleotides are listed in Table S3.

Sample preparation for ChIP-seq, data analysis, and visualization. ChIP and analysis of sequencing data were carried out as previously described (25), using Bowtie version 1.0.1 (61), SAMtools (62), the Integrative Genomics Viewer (IGV) (63), MEME (Multiple Expression Motifs [EM] for Motif Elicitation; <http://meme-suite.org/>) (64), TOMTOM (65), and the HOMER software for motif discovery and next-generation sequencing analysis (66).

EMSA. Gel shift assays were performed using oligonucleotides derived from ChIP-enriched regions and purified GST-PcVelA_{1–256}. Fifty-nucleotide double-stranded oligonucleotides (Table S3) were 5′-end labeled using polynucleotide kinase (Roche, Basel, Switzerland) and [γ -³²P]ATP (Hartmann Analytic, Braunschweig, Germany). For shift experiments, 3.5- to 7.0-fmol (~50 to 100 cps) samples of radiolabeled oligonucleotides were incubated with various protein concentrations in the presence of 2 μ l binding buffer (250 mM Tris-HCl, pH 8.0, 1 M KCl, 50% glycerol) and 1 μ g poly(dI-dC)-poly(dI-dC) (Affymetrix USB, CA, USA) in a total volume of 20 μ l for 20 min at room temperature. Samples were run on 5% polyacrylamide gels at 4°C in 190 mM glycine, 27 mM Tris-HCl, pH 8.5.

Expression, purification, and immunodetection of recombinant PcVelA-GST protein. Purification of recombinant PcVelA-GST protein from *E. coli* was performed as described earlier (67) using an elution buffer containing 50 mM Tris-HCl, 30 mM reduced glutathione, 100 mM NaCl, pH 8.0. Western blotting and immunodetection were performed using RPN1236 anti-GST horseradish peroxidase (HRP) conjugate (GE Healthcare, Germany).

Yeast two-hybrid analysis. Yeast two-hybrid analysis was carried out as described previously (13) using yeast strain PJ694a for GAL4 activation domain (AD) fusion derivatives and strain PJ69-4 α for Gal4 DNA binding domain (BD) fusion constructs.

Microscopy. Fluorescence and light microscopy were carried out as described previously (6, 68) with minor modifications. Images were captured with a Photometrics CoolSNAP HQ camera (Roper Scientific, USA) and MetaMorph (version 7.7.5.0; Universal Imaging). Recorded images were processed with MetaMorph and Adobe Photoshop CS4/CS6. Staining of nuclei was performed using DAPI (Sigma Aldrich, Germany). For analysis of conidiospore germination, *P. chrysogenum* strains were grown on solid CCM for 5 days at 27°C. For each strain, three biological replicates were analyzed. For each replicate, 100 conidiospores were analyzed.

Quantification of pellet diameter. For analysis of pellet formation, *P. chrysogenum* strains were grown for 72 h at 27°C and 120 rpm in CCM shaking cultures. Pictures were taken at $\times 6.35$ magnification, and interpretation was performed using the ImageJ software (<http://imagej.nih.gov/ij/index.html>).

Quantification of conidiation. Sporulation assays were performed as described previously (13) with some modifications. *P. chrysogenum* strains were grown on solid CCM, and incubation under light or dark conditions was performed for 120 h at 27°C.

Accession number(s). Raw sequencing data from ChIP-seq experiments are available from the NCBI SRA database under accession number [SRP067220](https://www.ncbi.nlm.nih.gov/sra/SRP067220).

SUPPLEMENTAL MATERIAL

Supplemental material for this article may be found at <http://dx.doi.org/10.1128/mSphere.00149-16>.

Figure S1, TIF file, 8.9 MB.

Figure S2, TIF file, 0.6 MB.

Figure S3, TIF file, 6.6 MB.

Figure S4, TIF file, 0.7 MB.

Figure S5, TIF file, 11.7 MB.

Figure S6, TIF file, 2.7 MB.

Data Set S1, XLSX file, 0.3 MB.

Table S1, PDF file, 0.05 MB.

Table S2, PDF file, 0.03 MB.

Table S3, PDF file, 0.02 MB.

ACKNOWLEDGMENTS

We thank M. Nowrousian and T. A. Dahlmann for help with bioinformatics and S. Mertens, I. Godehardt, K. Kalkreuter, and I. Schelberg for excellent technical assistance.

We further thank I. Zadra, H. Kürnsteiner, E. Friedlin, and T. Specht for their ongoing interest and support.

The authors declare no conflict of interests.

This work was funded by Sandoz GmbH (Kundl, Austria), the Christian Doppler Society (Vienna, Austria), the Studienstiftung des Deutschen Volkes (Bonn, Germany), and the Ruhr-University Bochum Research School (Bochum, Germany). The funders had no role in study design, data collection and interpretation, or the decision to submit the work for publication.

FUNDING INFORMATION

This work, including the efforts of Kordula Becker, Sandra Ziemons, Katharina Lentz, and Ulrich Kück, was funded by SANDOZ GmbH (Kundl, Austria). This work, including the efforts of Kordula Becker, Sandra Ziemons, Katharina Lentz, and Ulrich Kück, was funded by Christian Doppler Society (Vienna, Austria). This work, including the efforts of Kordula Becker, was funded by Ruhr University Bochum Research School (Bochum, Germany). This work, including the efforts of Kordula Becker, was funded by Studienstiftung des Deutschen Volkes (Bonn, Germany).

REFERENCES

- Barreiro C, Martín JF, García-Estrada C. 2012. Proteomics shows new faces for the old penicillin producer *Penicillium chrysogenum*. *J Biomed Biotechnol* **2012**:105109. <http://dx.doi.org/10.1155/2012/105109>.
- Fleming A. 1929. On the antibacterial action of cultures of a *Penicillium*, with special reference to their use in the isolation of *B. influenzae*. *Br J Exp Pathol* **10**:226–236.
- Peñalva MA, Rowlands RT, Turner G. 1998. The optimization of penicillin biosynthesis in fungi. *Trends Biotechnol* **16**:483–489. [http://dx.doi.org/10.1016/S0167-7799\(98\)01229-3](http://dx.doi.org/10.1016/S0167-7799(98)01229-3).
- Backus MP, Stauffer JF. 1955. The production and selection of a family of strains in *Penicillium chrysogenum*. *Mycologia* **47**:429–463. <http://dx.doi.org/10.2307/3755661>.
- Bayram Ö, Krappmann S, Ni M, Bok JW, Helmstaedt K, Valerius O, Braus-Stromeyer S, Kwon NJ, Keller NP, Yu JH, Braus GH. 2008. VelB/VeA/LaeA complex coordinates light signal with fungal development and secondary metabolism. *Science* **320**:1504–1506. <http://dx.doi.org/10.1126/science.1155888>.
- Hoff B, Kamerewerd J, Sigl C, Mitterbauer R, Zadra I, Kürnsteiner H, Kück U. 2010. Two components of a velvet-like complex control hyphal morphogenesis, conidiophore development, and penicillin biosynthesis in *Penicillium chrysogenum*. *Eukaryot Cell* **9**:1236–1250. <http://dx.doi.org/10.1128/EC.00077-10>.
- Wiemann P, Brown DW, Kleigrewe K, Bok JW, Keller NP, Humpf HU, Tudzynski B. 2010. FfVel1 and FfLae1, components of a velvet-like complex in *Fusarium fujikuroi*, affect differentiation, secondary metabolism and virulence. *Mol Microbiol* **77**:972–994. <http://dx.doi.org/10.1111/j.1365-2958.2010.07263.x>.
- Käfer E. 1965. Origins of translocations in *Aspergillus nidulans*. *Genetics* **52**:217–232.
- Kim H, Han K, Kim K, Han D, Jahng K, Chae K. 2002. The *veA* gene activates sexual development in *Aspergillus nidulans*. *Fungal Genet Biol* **37**:72–80. [http://dx.doi.org/10.1016/S1087-1845\(02\)00029-4](http://dx.doi.org/10.1016/S1087-1845(02)00029-4).
- Kato N, Brooks W, Calvo AM. 2003. The expression of sterigmatocystin and penicillin genes in *Aspergillus nidulans* is controlled by *veA*, a gene required for sexual development. *Eukaryot Cell* **2**:1178–1186. <http://dx.doi.org/10.1128/EC.2.6.1178-1186.2003>.
- Merhej J, Urban M, Dufresne M, Hammond-Kosack KE, Richard-Forget F, Barreau C. 2012. The velvet gene, *Fgve1*, affects fungal development and positively regulates trichothecene biosynthesis and pathogenicity in *Fusarium graminearum*. *Mol Plant Pathol* **13**:363–374. <http://dx.doi.org/10.1111/j.1364-3703.2011.00755.x>.
- Dreyer J, Eichhorn H, Friedlin E, Kürnsteiner H, Kück U. 2007. A homologue of the *Aspergillus* velvet gene regulates both cephalosporin C biosynthesis and hyphal fragmentation in *Acremonium chrysogenum*. *Appl Environ Microbiol* **73**:3412–3422. <http://dx.doi.org/10.1128/AEM.00129-07>.
- Kopke K, Hoff B, Bloemendal S, Katschorowski A, Kamerewerd J, Kück U. 2013. Members of the *Penicillium chrysogenum* velvet complex play functionally opposing roles in the regulation of penicillin biosynthesis and conidiation. *Eukaryot Cell* **12**:299–310. <http://dx.doi.org/10.1128/EC.00272-12>.
- Bok JW, Keller NP. 2004. LaeA, a regulator of secondary metabolism in *Aspergillus* spp. *Eukaryot Cell* **3**:527–535. <http://dx.doi.org/10.1128/EC.3.2.527-535.2004>.
- Sarikaya Bayram Ö, Bayram Ö, Valerius O, Park HS, Irniger S, Gerke J, Ni M, Han KH, Yu JH, Braus GH. 2010. LaeA control of velvet family regulatory proteins for light-dependent development and fungal cell-type specificity. *PLoS Genet* **6**:e1001226. <http://dx.doi.org/10.1371/journal.pgen.1001226>.
- Ni M, Yu JH. 2007. A novel regulator couples sporogenesis and trehalose biogenesis in *Aspergillus nidulans*. *PLoS One* **2**:e970. <http://dx.doi.org/10.1371/journal.pone.0000970>.
- Lind AL, Wisecaver JH, Smith TD, Feng X, Calvo AM, Rokas A. 2015. Examining the evolution of the regulatory circuit controlling secondary metabolism and development in the fungal genus *Aspergillus*. *PLoS Genet* **11**:e1005096. <http://dx.doi.org/10.1371/journal.pgen.1005096>.
- Beyhan S, Gutierrez M, Voorhies M, Sil A. 2013. A temperature-responsive network links cell shape and virulence traits in a primary fungal pathogen. *PLoS Biol* **11**:e1001614. <http://dx.doi.org/10.1371/journal.pbio.1001614>.
- Ahmed YL, Gerke J, Park HS, Bayram Ö, Neumann P, Ni M, Dickmanns A, Kim SC, Yu JH, Braus GH, Ficner R. 2013. The velvet family of fungal regulators contains a DNA-binding domain structurally similar to NF-κB. *PLoS Biol* **11**:e1001750. <http://dx.doi.org/10.1371/journal.pbio.1001750>.
- Smith KM, Sancar G, Dekhang R, Sullivan CM, Li S, Tag AG, Sancar C, Bredeweg EL, Priest HD, McCormick RF, Thomas TL, Carrington JC, Stajich JE, Bell-Pedersen D, Brunner M, Freitag M. 2010. Transcription factors in light and circadian clock signaling networks revealed by genomewide mapping of direct targets for *Neurospora* white collar complex. *Eukaryot Cell* **9**:1549–1556. <http://dx.doi.org/10.1128/EC.00154-10>.
- Gao F, Foat BC, Bussemaker HJ. 2004. Defining transcriptional networks through integrative modeling of mRNA expression and transcription factor binding data. *BMC Bioinformatics* **5**:31. <http://dx.doi.org/10.1186/1471-2105-5-31>.
- Sandmann T, Jensen LJ, Jakobsen JS, Karzynski MM, Eichenlaub MP, Bork P, Furlong EEM. 2006. A temporal map of transcription factor activity: Mef2 directly regulates at all stages of muscle target genes development. *Dev Cell* **10**:797–807. <http://dx.doi.org/10.1016/j.devcel.2006.04.009>.
- Jakobsen JS, Braun M, Astorga J, Gustafson EH, Sandmann T, Karzynski M, Carlsson P, Furlong EE. 2007. Temporal ChIP-on-chip reveals Biniou as a universal regulator of the visceral muscle transcriptional network. *Genes Dev* **21**:2448–2460. <http://dx.doi.org/10.1101/gad.437607>.
- Vokes SA, Ji H, Wong WH, McMahon AP. 2008. A genome-scale analysis of the *cis*-regulatory circuitry underlying sonic hedgehog-

- mediated patterning of the mammalian limb. *Genes Dev* **22**:2651–2663. <http://dx.doi.org/10.1101/gad.1693008>.
25. **Becker K, Beer C, Freitag M, Kück U.** 2015. Genome-wide identification of target genes of a mating-type α -domain transcription factor reveals functions beyond sexual development. *Mol Microbiol* **96**:1002–1022. <http://dx.doi.org/10.1111/mmi.12987>.
 26. **Adams TH, Boylan MT, Timberlake WE.** 1988. BrlA is necessary and sufficient to direct conidiophore development in *Aspergillus nidulans*. *Cell* **54**:353–362. [http://dx.doi.org/10.1016/0092-8674\(88\)90198-5](http://dx.doi.org/10.1016/0092-8674(88)90198-5).
 27. **Arratia-Quijada J, Sánchez O, Sczzocchio C, Aguirre J.** 2012. FlbD, a Myb transcription factor of *Aspergillus nidulans*, is uniquely involved in both asexual and sexual differentiation. *Eukaryot Cell* **11**:1132–1142. <http://dx.doi.org/10.1128/EC.00101-12>.
 28. **Kraus PR, Hofmann AF, Harris SD.** 2002. Characterization of the *Aspergillus nidulans* 14-3-3 homologue, ArtA. *FEMS Microbiol Lett* **210**:61–66. <http://dx.doi.org/10.1111/j.1574-6968.2002.tb11160.x>.
 29. **Kwon NJ, Garzia A, Espeso EA, Ugalde U, Yu JH.** 2010. FlbC is a putative nuclear C2H2 transcription factor regulating development in *Aspergillus nidulans*. *Mol Microbiol* **77**:1203–1219. <http://dx.doi.org/10.1111/j.1365-2958.2010.07282.x>.
 30. **Olmedo M, Ruger-Herreros C, Luque EM, Corrochano LM.** 2010. A complex photoreceptor system mediates the regulation by light of the conidiation genes *con-10* and *con-6* in *Neurospora crassa*. *Fungal Genet Biol* **47**:352–363. <http://dx.doi.org/10.1016/j.fgb.2009.11.004>.
 31. **D'Enfert C, Fontaine T.** 1997. Molecular characterization of the *Aspergillus nidulans* *treA* gene encoding an acid trehalase required for growth on trehalose. *Mol Microbiol* **24**:203–216. <http://dx.doi.org/10.1046/j.1365-2958.1997.3131693.x>.
 32. **Stringer MA, Timberlake WE.** 1995. *dewA* encodes a fungal hydrophobin component of the *Aspergillus* spore wall. *Mol Microbiol* **16**:33–44. <http://dx.doi.org/10.1111/j.1365-2958.1995.tb02389.x>.
 33. **Goyal K, Walton LJ, Tunnacliffe A.** 2005. LEA proteins prevent protein aggregation due to water stress. *Biochem J* **388**:151–157. <http://dx.doi.org/10.1042/BJ20041931>.
 34. **Sigl C, Haas H, Specht T, Pfaller K, Kürnsteiner H, Zadra I.** 2011. Among developmental regulators, StuA but not BrlA is essential for penicillin V production in *Penicillium chrysogenum*. *Appl Environ Microbiol* **77**:972–982. <http://dx.doi.org/10.1128/AEM.01557-10>.
 35. **Miller KY, Wu J, Miller BL.** 1992. StuA is required for cell pattern-formation in *Aspergillus*. *Genes Dev* **6**:1770–1782. <http://dx.doi.org/10.1101/gad.6.9.1770>.
 36. **Todeschini AL, Georges A, Veitia RA.** 2014. Transcription factors: specific DNA binding and specific gene regulation. *Trends Genet* **30**: 211–219. <http://dx.doi.org/10.1016/j.tig.2014.04.002>.
 37. **Milam AH, Rose L, Cideciyan AV, Barakat MR, Tang WX, Gupta N, Aleman TS, Wright AF, Stone EM, Sheffield VC, Jacobson SG.** 2002. The nuclear receptor NR2E3 plays a role in human retinal photoreceptor differentiation and degeneration. *Proc Natl Acad Sci U S A* **99**:473–478. <http://dx.doi.org/10.1073/pnas.022533099>.
 38. **Kobayashi M, Takezawa S, Hara K, Yu RT, Umesono Y, Agata K, Taniwaki M, Yasuda K, Umesono K.** 1999. Identification of a photoreceptor cell-specific nuclear receptor. *Proc Natl Acad Sci U S A* **96**: 4814–4819. <http://dx.doi.org/10.1073/pnas.96.9.4814>.
 39. **Bosch DG, Boonstra FN, Gonzaga-Jauregui C, Xu M, de Ligt J, Jhangiani S, Wiszniewski W, Muzny DM, Yntema HG, Pfundt R, Vissers LE, Spruijt L, Blokland EA, Chen CA, Lewis RA, Tsai SY, Gibbs RA, Tsai MJ, Lupski JR, Zoghbi HY, Cremers FP, de Vries BB, Schaaf CP.** 2014. NR2F1 mutations cause optic atrophy with intellectual disability. *Am J Hum Genet* **94**:303–309. <http://dx.doi.org/10.1016/j.ajhg.2014.01.002>.
 40. **Palmer JM, Theisen JM, Duran RM, Grayburn WS, Calvo AM, Keller NP.** 2013. Secondary metabolism and development is mediated by LlmF control of VeA subcellular localization in *Aspergillus nidulans*. *PLoS Genet* **9**:e1003193. <http://dx.doi.org/10.1371/journal.pgen.1003193>.
 41. **Sarikaya-Bayram Ö, Bayram Ö, Feussner K, Kim JH, Kim HS, Kaever A, Feussner I, Chae KS, Han DM, Han KH, Braus GH.** 2014. Membrane-bound methyltransferase complex VapA-VipC-VapB guides epigenetic control of fungal development. *Dev Cell* **29**:406–420. <http://dx.doi.org/10.1016/j.devcel.2014.03.020>.
 42. **Jiang J, Liu X, Yin Y, Ma Z.** 2011. Involvement of a velvet protein FgVeA in the regulation of asexual development, lipid and secondary metabolisms and virulence in *Fusarium graminearum*. *PLoS One* **6**:e28291. <http://dx.doi.org/10.1371/journal.pone.0028291>.
 43. **Kagan RM, Clarke S.** 1994. Widespread occurrence of three sequence motifs in diverse S-adenosylmethionine-dependent methyltransferases suggests a common structure for these enzymes. *Arch Biochem Biophys* **310**:417–427. <http://dx.doi.org/10.1006/abbi.1994.1187>.
 44. **Hacker C, Glinski M, Hornbogen T, Doller A, Zocher R.** 2000. Mutational analysis of the N-methyltransferase domain of the multifunctional enzyme enniatin synthetase. *J Biol Chem* **275**:30826–30832. <http://dx.doi.org/10.1074/jbc.M002614200>.
 45. **Kozbial PZ, Mushegian AR.** 2005. Natural history of S-adenosylmethionine-binding proteins. *BMC Struct Biol* **5**:19. <http://dx.doi.org/10.1186/1472-6807-5-19>.
 46. **Martin JL, McMillan FM.** 2002. SAM (dependent) I AM: the S-adenosylmethionine-dependent methyltransferase fold. *Curr Opin Struct Biol* **12**:783–793. [http://dx.doi.org/10.1016/S0959-440X\(02\)00391-3](http://dx.doi.org/10.1016/S0959-440X(02)00391-3).
 47. **Yang J, Yan R, Roy A, Xu D, Poisson J, Zhang Y.** 2015. The I-TASSER suite: protein structure and function prediction. *Nat Methods* **12**:7–8. <http://dx.doi.org/10.1038/nmeth.3213>.
 48. **Roy A, Kucukural A, Zhang Y.** 2010. I-TASSER: a unified platform for automated protein structure and function prediction. *Nat Protoc* **5**:725–738. <http://dx.doi.org/10.1038/nprot.2010.5>.
 49. **Zhang Y.** 2008. I-TASSER server for protein 3D structure prediction. *BMC Bioinformatics* **9**:40. <http://dx.doi.org/10.1186/1471-2105-9-40>.
 50. **Hoff B, Kück U.** 2005. Use of bimolecular fluorescence complementation to demonstrate transcription factor interaction in nuclei of living cells from the filamentous fungus *Acremonium chrysogenum*. *Curr Genet* **47**:132–138. <http://dx.doi.org/10.1007/s00294-004-0546-0>.
 51. **Hedtke M, Rauscher S, Röhrig J, Rodríguez-Romero J, Yu Z, Fischer R.** 2015. Light-dependent gene activation in *Aspergillus nidulans* is strictly dependent on phytochrome and involves the interplay of phytochrome and white collar-regulated histone H3 acetylation. *Mol Microbiol* **97**:733–745. <http://dx.doi.org/10.1111/mmi.13062>.
 52. **Sarikaya-Bayram Ö, Palmer JM, Keller N, Braus GH, Bayram Ö.** 2015. One Juliet and four Romeos: VeA and its methyltransferases. *Front Microbiol* **6**:1. <http://dx.doi.org/10.3389/fmicb.2015.00001>.
 53. **Struck AW, Thompson ML, Wong LS, Micklefield J.** 2012. S-adenosylmethionine-dependent methyltransferases: highly versatile enzymes in biocatalysis, biosynthesis and other biotechnological applications. *ChemBiochem* **13**:2642–2655. <http://dx.doi.org/10.1002/cbic.201200556>.
 54. **Wolfers S, Kamerewerd J, Nowrousian M, Sigl C, Zadra I, Kürnsteiner H, Kück U, Bloemendal S.** 2015. Microarray hybridization analysis of light-dependent gene expression in *Penicillium chrysogenum* identifies bZIP transcription factor PcAtfA. *J Basic Microbiol* **55**:480–489. <http://dx.doi.org/10.1002/jobm.201400588>.
 55. **Bullock WO, Fernandez JM, Short JM.** 1987. X11-blue—a high-efficiency plasmid transforming *recA* *Escherichia coli* strain with β -galactosidase selection. *Biotechniques* **5**:376–378.
 56. **Miroux B, Walker JE.** 1996. Over-production of proteins in *Escherichia coli*: mutant hosts that allow synthesis of some membrane proteins and globular proteins at high levels. *J Mol Biol* **260**:289–298. <http://dx.doi.org/10.1006/jmbi.1996.0399>.
 57. **James P, Halladay J, Craig EA.** 1996. Genomic libraries and a host strain designed for highly efficient two-hybrid selection in yeast. *Genetics* **144**:1425–1436.
 58. **Kamerewerd J, Zadra I, Kürnsteiner H, Kück U.** 2011. Pch1B1, encoding a class V chitinase, is affected by PcVeA and PcLaeA, and is responsible for cell wall integrity in *Penicillium chrysogenum*. *Microbiology* **157**:3036–3048. <http://dx.doi.org/10.1099/mic.0.051896-0>.
 59. **Hoff B, Kamerewerd J, Sigl C, Zadra I, Kück U.** 2010. Homologous recombination in the antibiotic producer *Penicillium chrysogenum*: strain Δ Pcku70 shows up-regulation of genes from the HOG pathway. *Appl Microbiol Biotechnol* **85**:1081–1094. <http://dx.doi.org/10.1007/s00253-009-2168-4>.
 60. **Böhm J, Hoff B, O'Gorman CM, Wolfers S, Kliks V, Binger D, Zadra I, Kürnsteiner H, Pöggeler S, Dyer PS, Kück U.** 2013. Sexual reproduction and mating-type-mediated strain development in the penicillin-producing fungus *Penicillium chrysogenum*. *Proc Natl Acad Sci U S A* **110**:1476–1481. <http://dx.doi.org/10.1073/pnas.1217943110>.
 61. **Langmead B, Trapnell C, Pop M, Salzberg SL.** 2009. Ultrafast and memory-efficient alignment of short DNA sequences to the human genome. *Genome Biol* **10**:R25. <http://dx.doi.org/10.1186/gb-2009-10-3-r25>.
 62. **Li H, Handsaker B, Wysoker A, Fennell T, Ruan J, Homer N, Marth G, Abecasis G, Durbin R, 1000 Genome Project Data Processing Subgroup.** 2009. The Sequence Alignment/Map format and SAMtools. *Bioin-*

- formatics **25**:2078–2079. <http://dx.doi.org/10.1093/bioinformatics/btp352>.
63. **Thorvaldsdóttir H, Robinson JT, Mesirov JP.** 2013. Integrative genomics viewer (IGV): high-performance genomics data visualization and exploration. *Brief Bioinform* **14**:178–192. <http://dx.doi.org/10.1093/bib/bbs017>.
 64. **Bailey TL, Elkan C.** 1994. Fitting a mixture model by expectation maximization to discover motifs in biopolymers. *Proc Int Conf Intell Syst Mol Biol* **2**:28–36.
 65. **Gupta S, Stamatoyannopoulos JA, Bailey TL, Noble WS.** 2007. Quantifying similarity between motifs. *Genome Biol* **8**:R24. <http://dx.doi.org/10.1186/gb-2007-8-2-r24>.
 66. **Heinz S, Benner C, Spann N, Bertolino E, Lin YC, Laslo P, Cheng JX, Murre C, Singh H, Glass CK.** 2010. Simple combinations of lineage-determining transcription factors prime *cis*-regulatory elements required for macrophage and B cell identities. *Mol Cell* **38**:576–589. <http://dx.doi.org/10.1016/j.molcel.2010.05.004>.
 67. **Janus D, Hortschansky P, Kück U.** 2008. Identification of a minimal *cre1* promoter sequence promoting glucose-dependent gene expression in the β -lactam producer *Acremonium chrysogenum*. *Curr Genet* **53**:35–48. <http://dx.doi.org/10.1007/s00294-007-0164-8>.
 68. **Engh I, Würtz C, Witzel-Schlömp K, Zhang HY, Hoff B, Nowrousian M, Rottensteiner H, Kück U.** 2007. The WW domain protein PRO40 is required for fungal fertility and associates with woronin bodies. *Eukaryot Cell* **6**:831–843. <http://dx.doi.org/10.1128/EC.00269-06>.
 69. **Hagiwara D, Suzuki S, Kamei K, Gono T, Kawamoto S.** 2014. The role of AtfA and HOG MAPK pathway in stress tolerance in conidia of *Aspergillus fumigatus*. *Fungal Genet Biol* **73**:138–149. <http://dx.doi.org/10.1016/j.fgb.2014.10.011>.
 70. **Balázs A, Pócsi I, Hamari Z, Leiter E, Emri T, Miskei M, Oláh J, Tóth V, Hegedus N, Prade RA, Molnár M, Pócsi I.** 2010. AtfA bZIP-type transcription factor regulates oxidative and osmotic stress responses in *Aspergillus nidulans*. *Mol Genet Genomics* **283**:289–303. <http://dx.doi.org/10.1007/s00438-010-0513-z>.
 71. **DeZwaan TM, Carroll AM, Valent B, Sweigard JA.** 1999. *Magnaporthe grisea* Pth11p is a novel plasma membrane protein that mediates appressorium differentiation in response to inductive substrate cues. *Plant Cell* **11**:2013–2030. <http://dx.doi.org/10.1105/tpc.11.10.2013>.
 72. **Chakrabortee S, Tripathi R, Watson M, Schierle GSK, Kurniawan DP, Kaminski CF, Wise MJ, Tunnacliffe A.** 2012. Intrinsically disordered proteins as molecular shields. *Mol Biosyst* **8**:210–219. <http://dx.doi.org/10.1039/c1mb05263b>.